

Redox reaction between $[\text{Bu}_4\text{N}]_2[\text{Mo}^{\text{VI}}\text{O}_2(\text{mnt})_2]$ and thiophenol in relevance to the autoreduction in the crystallization process of oxidized form of sulfite oxidase

Pradeep K Chaudhury^a, Kowliki Nagarajan^b, Anil Kumar^b, Rabindranath Maiti^c, Samar K Das^d & Sabyasachi Sarkar^{b*}

^aDepartment of Chemistry, University of Pune, Pune, India

^bDepartment of Chemistry, Indian Institute of Technology, Kanpur 208 016, India Email:abya@iitk.ac.in

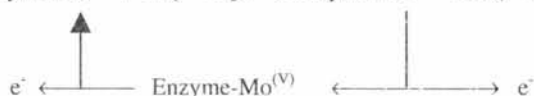
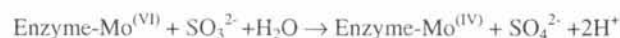
^cIndian Institute of Technology Kharagpur, Kharagpur, India

^dDepartment of Chemistry, Central University of Hyderabad, Hyderabad, India

Received 3 February 2003

$[\text{Bu}_4\text{N}]_2[\text{Mo}^{\text{VI}}\text{O}_2(\text{mnt})_2]$ readily reacts with thiophenol leading to its reduction to $[\text{Bu}_4\text{N}]_2[\text{Mo}^{\text{IV}}\text{O}(\text{mnt})_2]$. Detailed kinetics of this reaction is presented. The kinetics consists of three consecutive irreversible first order reactions (in the presence of excess of thiophenol) with $k_1, k_2, k_3 = 2.82(6) \times 10^{-1} \text{ s}^{-1}, 6.09(5) \times 10^{-2} \text{ s}^{-1}, 1.66(8) \times 10^{-3} \text{ s}^{-1}$ and $2.91(4) \times 10^{-1} \text{ s}^{-1}, 6.15(3) \times 10^{-2} \text{ s}^{-1}, 3.41(6) \times 10^{-3} \text{ s}^{-1}$ at 298 K in acetonitrile and aqueous-acetonitrile media respectively.

Sulfite oxidase catalyzes physiologically vital oxidation of sulfite to sulfate¹. The enzyme residing in the mitochondrial inter-membrane space, is dimeric with a subunit mass of about 52000. Each monomer contains molybdenum associated with a single molybdopterin and a cytochrome *b* type heme. The two electron oxidation of sulfite to sulfate is known to occur at the molybdenum site, which is reduced from Mo(VI) to Mo(IV) in the process, and the catalytic cycle is completed with the reoxidation of the molybdenum in sequential two one electron transfer reactions {Mo(IV)-Mo(V)-Mo(VI)} associated with intramolecular electron transfer to the cytochrome *b* site²:



With the exception of nitrogenase, all molybdenum enzymes that have been described to date³ contain a novel pterin cofactor in which the molybdenum is bound by the pyranodithiolene of the molybdopterin cofactor^{3,4} (Fig. 1).

Until recently, structural information on molybdenum enzymes was derived almost entirely from spectroscopy of the enzyme and of model compounds³. As one of the most intensively studied molybdenum enzymes, sulfite oxidase can be

regarded as prototypical member of one class of molybdenum enzymes—those possessing dioxo molybdenum sites when the enzyme is in the fully oxidized Mo(VI) form⁵⁻⁸. Recently, the crystal structure of chicken liver sulfite oxidase has been reported at 1.9 Å resolution⁹. In contrast to the information available from previous X-ray absorption spectroscopic studies, the active site as revealed by crystallography was found to contain monoxo species where molybdenum is in the reduced {Mo(IV)} state. Although the X-ray diffraction quality crystals were grown from the fully oxidized state of the protein (Fig. 2a), its reduction to Mo(IV) state (Fig. 2b) has been attributed presumably to long standing in the presence of by trace amounts of sulfite present in the precipitant, lithium sulfate, used in such crystallization processes.

Our model complex containing bis-dithiolene coordination in $[\text{Bu}_4\text{N}]_2[\text{MoO}_2(\text{mnt})_2]$ (**1**) uniquely mimics enzymatic reaction of sulfite oxidase¹⁰. In this

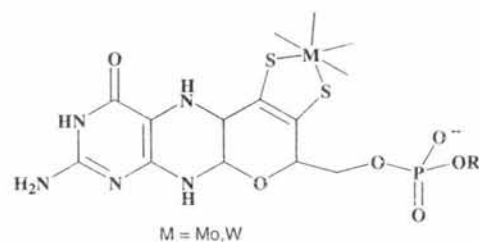


Fig. 1—The minimal coordination unit of a molybdenum cofactor, showing the structure of molybdopterin (MPT).

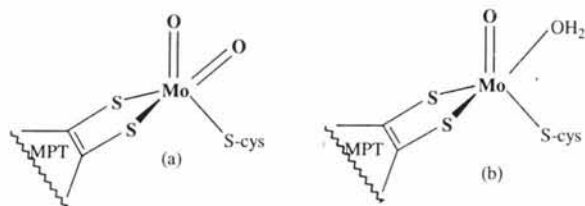


Fig. 2—Schematic structures of the molybdenum active site of sulfite oxidase from (a) X-ray absorption spectroscopy of oxidized enzyme and from (b) crystallography. The coordinated water in (b) might alternatively be a hydroxyl.

model complex, molybdenum core $\{\text{Mo}^{\text{VI}}\text{O}_2\}^{2+}$ is stabilized by two dithiolene moiety whereas in native enzyme it is stabilized by one dithiolene (MPT) and one thiolate (cysteine) ligation. The chemistry involved in the crystallization process is intriguing since the isolated single crystal was found to be in the reduced form $\{\text{Mo}(\text{IV})\}$ although the crystals were allowed to grow from fully oxidized state $\{\text{Mo}(\text{VI})\}$ of the protein. The present paper is related to similar chemistry as we have shown that $[\text{Bu}_4\text{N}]_2[\text{Mo}^{\text{VI}}\text{O}_2(\text{mnt})_2]$ readily reacts with thiol leading its reduction to $[\text{Mo}^{\text{IV}}\text{O}(\text{mnt})_2]^{2-}$.

Materials and Methods

The complex, $[\text{Bu}_4\text{N}]_2[\text{Mo}^{\text{VI}}\text{O}_2(\text{mnt})_2]$ (**1**) was prepared according to the published procedure¹⁰. AR grade thiophenol (Lancaster) was used as received. Acetonitrile was purified and dried by standard methods. Double distilled water was used for the kinetic experiments. UV-visible electronic spectra were recorded on Shimadzu 160 and Cintra 10 GBC UV-visible spectrophotometers. Infra red spectrum was recorded as KBr pellets on Perkin Elmer 577. Cyclic voltammetric measurements were made with CV-27 BAS Bioanalytical Systems using 10^{-3} M solutions of the compound by glassy carbon working electrode, Ag/AgCl reference electrode, platinum wire auxiliary electrode and $[\text{Et}_4\text{N}]\text{ClO}_4$ as supporting electrolyte.

The reaction between $[\text{MoO}_2(\text{mnt})_2]^{2-}$ and PhSH was carried out in preparative scale as described below where the reaction proceeded almost in quantitative yield.

Reaction between $[\text{MoO}_2(\text{mnt})_2]^{2-}$ and PhSH

A solution of 1 mmol of $[\text{Bu}_4\text{N}]_2[\text{MoO}_2(\text{mnt})_2]$ (**1**) (0.89 g) in 10 ml acetonitrile was treated with 5 mmol of PhSH (0.5 ml). The solution was kept overnight at room temperature, the initial reddish brown colored

solution changed to greenish brown over this period of time. Addition of 10 ml isopropanol and 10 ml diethylether caused the precipitation of a dirty-green solid. Analysis of the solid proved that it is $[\text{Bu}_4\text{N}]_2[\text{MoO}(\text{mnt})_2]$ (**4**)¹⁰. [Yield: 0.78g (90%). Anal.: Found (Calcd.): C 54.70(54.76), H 8.32(8.27), N 9.66(9.58), S 14.60(14.62). IR data: $\nu(\text{Mo}=\text{O})=928\text{cm}^{-1}$, $\nu(\text{CN})=2194\text{cm}^{-1}$, $\nu(\text{C}=\text{C})_{\text{dithiolene}}=1482\text{cm}^{-1}$. UV-visible data: $\lambda_{\text{max, nm}} (\epsilon, \text{M}^{-1}\text{cm}^{-1})$: 602 (110), 491(187), 395 (sh), 363 (10055) in acetonitrile].

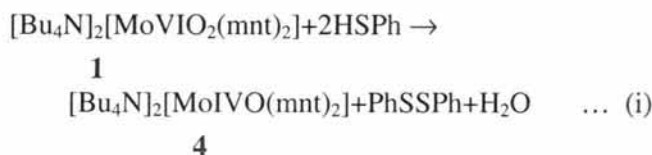
Kinetic measurements

All the kinetic measurements were carried out with Shimadzu 160 spectrophotometer provided with a piezoelectric thermostating device for the regulation of temperature. In a typical experiment a stock solution of complex (**1**) of required concentration was taken in the cell (path length 1cm) fitted with a serum cap and placed in the cell compartment. After thermal equilibration the reactant (thiophenol solution) solution of known concentration was added to the cell solution by a calibrated syringe and the cell contents were quickly mixed. The progress of the reaction was monitored by the change in absorbance at 610 nm with time. Duplicate kinetic runs were made for each reaction.

Results and Discussions

Nature of the reaction

UV-visible spectroscopy—The reaction between $[\text{Mo}^{\text{VI}}\text{O}_2(\text{mnt})_2]^{2-}$ and PhSH is as depicted below



Progress of the reaction (i) when followed spectrophotometrically showed a gradual decrease in the intensity of 525 nm band of **1** (Fig. 3). The same reaction when monitored using 10 times more concentration of the complex as well as of thiophenol, the repetitive scan at a lesser time interval for the initial phase of the reaction showed continuous development of the band at 610 nm with an isosbestic point at 570 nm for about 2.5 minutes (Fig. 4a). After the lapse of 3 min., decrease in the absorption between 450-650 nm with the loss of isosbesticity (Fig. 4b) was observed. This observation clearly suggests that reduction of **1** to **4** does not take place

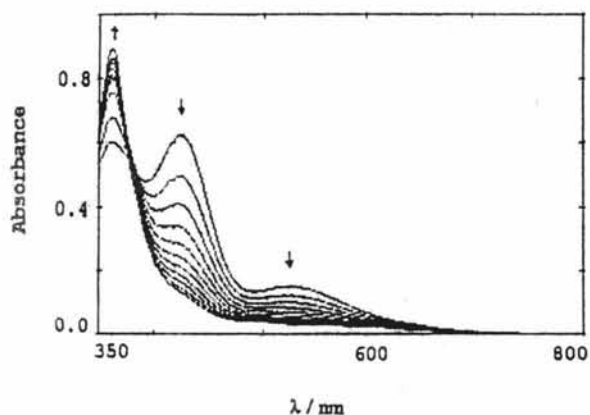


Fig. 3—Spectral changes for the reaction between **1** ($1 \times 10^{-4} M$) and PhSH ($5 \times 10^{-2} M$) in acetonitrile, scan 8 hours; 30 min/scan.

directly rather it proceeds through one or more than one intermediates.

Cyclic voltammetry—In order to have a better understanding about the mechanistic aspect of reaction (i), cyclic voltammetric studies were carried with the assumption that the intermediate species should display different electrochemical response. The cyclic voltammogram of **1** ($1 \times 10^{-3} M$) in the presence of HSPh ($0.5 M$) in acetonitrile was recorded and the following observations were made:

Quasireversible reduction peak potential of **1** centered at $-1.10 V$ vs. Ag/AgCl with cathodic peak potential at $-1.15 V$ in the presence of thiophenol became irreversible with the appearance of cathodic peak potential at $-0.99 V$ vs Ag/AgCl. Further, repetitive scans of this solution displayed the appearance of $\{\text{Mo}^{\text{V}}\text{O}\}/\{\text{Mo}^{\text{IV}}\text{O}\}$ couple on the positive side after about 3 minutes with the gradual fall in current for E_{pc} at $-0.99 V$. This suggests the formation of **4** (Scheme 1) from the species which has E_{pc} at $-0.99 V$ (Fig. 5a). To check the formation of any intermediate redox active species the voltammogram was recorded with low concentration of PhSH. The acetonitrile used for this purpose was not dried prior to its use. With low concentration of PhSH ($1.0 \times 10^{-2} M$), **1** displayed three cathodic peak potentials at $-0.99 V$, $-1.05 V$ and $-1.13 V$ vs Ag/AgCl (Fig. 5b). **1** in aquated acetonitrile (5% *v/v*) showed the shift of E_{pc} from $-1.15 V$ to $-1.13 V$ presumably due to hydrogen bonding with cyano groups of ligated “mnt” causing drift of the electron density away from the molybdenum center and thus causing its reduction easier. Hence the E_{pc} at $-1.13 V$ is due to the formation of hydrogen bonding of the peripheral cyano group of

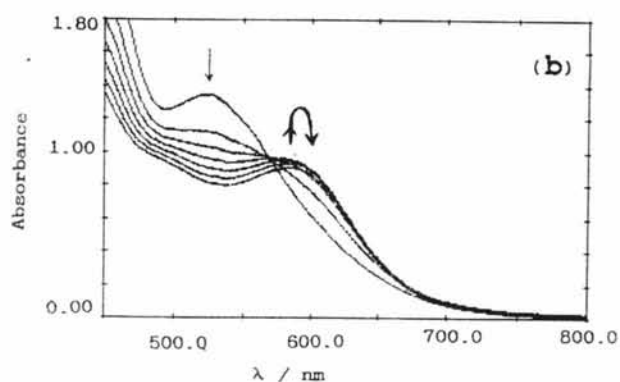
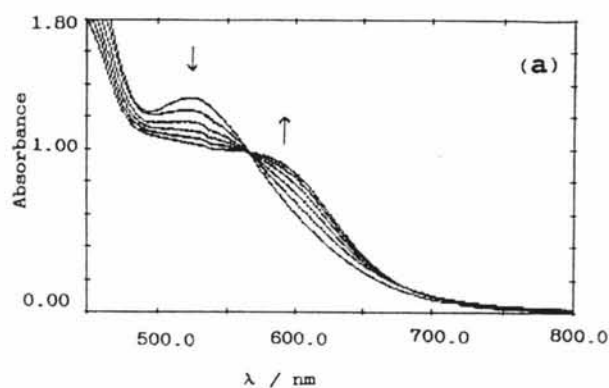
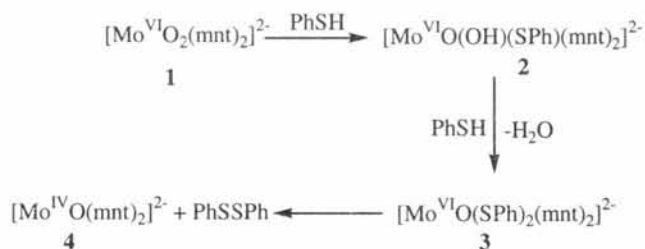


Fig. 4—Spectral changes for the reaction between **1** ($1 \times 10^{-3} M$) and PhSH ($5 \times 10^{-1} M$) in acetonitrile [Expanded form: (a) initial phase of the reaction for first 2.5 min (scan interval 30 sec) shows isosbestic point at 570 nm; (b) after the lapse of 3 min it shows the disappearance of the isosbestic point (scan interval one min)].



Scheme 1

coordinated mnt in species **1**. Similar effect with peripheral cyano ligand is known¹¹. Gradual addition of more amount of HSPh to **1** led to the decrease in current of E_{pc} at $-1.13 V$ with the increase in current for E_{pc} at $-0.99 V$ and the appearance of E_{pc} at $-1.05 V$ as a shoulder was observed. Cyclic voltammetric data

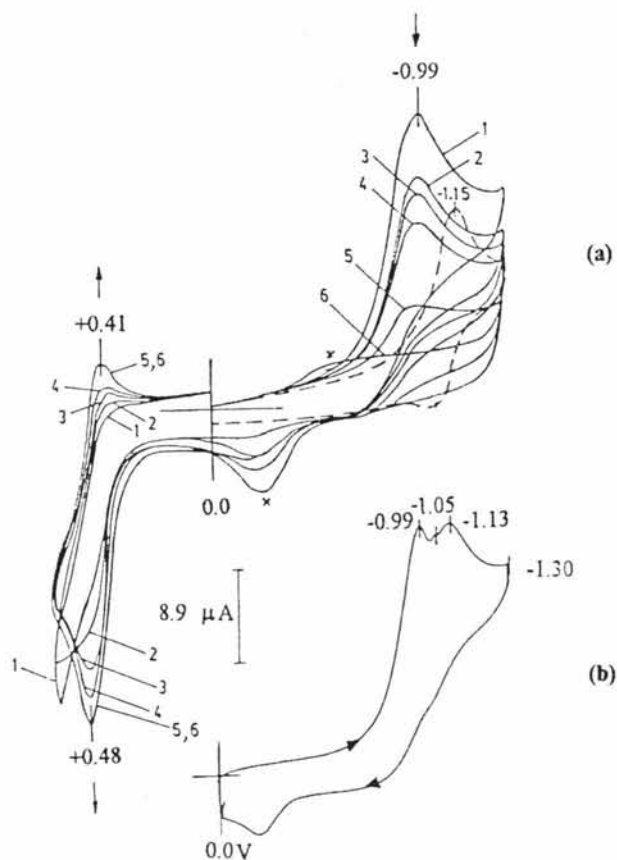


Fig. 5—(a) Cyclic voltammograms for the progress of the reaction between **1** ($1 \times 10^{-3} M$) and PhSH ($5 \times 10^{-1} M$) in acetonitrile, $0.1 M$ Et_4NClO_4 , scan rate $[100 \text{ mV/s}]$. Broken line is for pure complex (**1**). Each scan (1-6) in 5 min interval, \times marked peaks are unidentified; (b) Cyclic voltammogram for the same reaction at **1**: PhSH ($10^{-3}:10^{-2} M$).

with low concentration ($1.0 \times 10^{-2} M$) of HSPH is in fact indicative of the formation of two intermediates (**2,3**) rather than one as shown in Scheme 1. Thus the cathodic peak potentials at -1.13 V , -1.05 V and -0.99 V can be attributed to the species **1**, **2** and **3** respectively (Scheme 1). This is supported by increase in the absorbance profile at 610 nm for the earlier phase of the reaction (i) with an isosbestic point at 570 nm and the loss of isosbesticity during later phase of the reaction (Fig. 4 a&b). The reaction between **1** and PhSH did not show any EPR active species for the entire course of the reaction suggesting no involvement of stepwise one-electron redox reaction. The formation of **4** from **3** (Scheme 1) may be viewed as a reductive elimination process wherein hepta coordinated Mo(VI) is spontaneously changed to penta coordinated Mo(IV) species. Once **4** is formed it responds to known one electron oxidation reaction

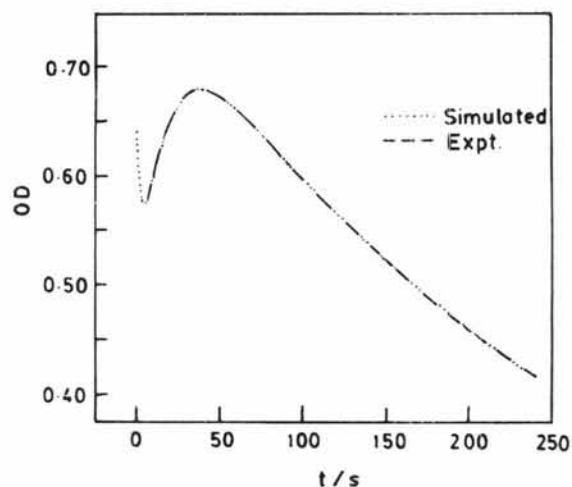
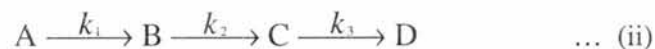


Fig. 6—Experimentally observed and simulated kinetic traces at 610 nm (Table 1) in aqueous acetonitrile medium.

(Fig. 5a). Based on the above discussion the following mechanism has been proposed for reaction (i) (Scheme 1).

Kinetics of reaction (i)

The kinetics of the reaction (i) was carried out spectrophotometrically in acetonitrile as well as in aqueous-acetonitrile media following the change of absorbance at 610 nm . As a representative example the kinetic trace in aqueous-acetonitrile is given in Fig. 6. The kinetic data fitted well to the consecutive reaction scheme given in Eq. (ii) for the reaction (i) both in acetonitrile as well as in aqueous acetonitrile media when the composite OD (at 610 nm) at time t was taken to be the sum of the contributions from the species A, B, C, D of Eq. (ii) as given by Eq. (iii).



$$\text{OD}(610) = \epsilon_1 C_A + \epsilon_2 C_B + \epsilon_3 C_C + \epsilon_4 C_D \quad \dots \text{ (iii)}$$

(where $\epsilon_1, \epsilon_2, \epsilon_3, \epsilon_4$ are molar extinction coefficients of A, B, C, D respectively).

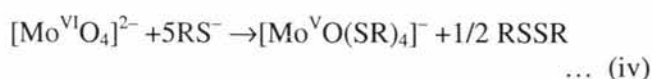
The analytical solutions for C_A, C_B, C_C and C_D of the Eq. (ii) are well known¹². Eq. (iii) was solved for k_1, k_2, k_3 and ϵ_2 and ϵ_3 (ϵ_1 and ϵ_4 are known, see Table 1) by non-linear least-square regression analyses using E04FDF NAG Fortran library routine document¹³ and their values are given in Table 1. The simulated kinetic trace using the parameters entered in Table 1, when aqueous-acetonitrile was the medium, is also given in Fig. 6 for comparison with the experimentally obtained kinetic trace.

Table 1—Results of the kinetic experiment for the reaction (i)..

	In acetonitrile	In acetonitrile with 6.3% water
Compound conc. (1)	$1 \times 10^{-3} M$	$1 \times 10^{-3} M$
PhSH concentration	$3.25 \times 10^{-1} M$	$4.86 \times 10^{-1} M$
Temperature	25 (± 0.1) °C	25 (± 0.1) °C
k_1	$2.82 (6) \times 10^{-1} s^{-1}$	$2.91 (4) \times 10^{-1} s^{-1}$
k_2	$6.09 (5) \times 10^{-2} s^{-1}$	$6.15 (3) \times 10^{-2} s^{-1}$
k_3	$1.66 (8) \times 10^{-3} s^{-1}$	$3.41 (6) \times 10^{-3} s^{-1}$
ϵ_1	$580.0 M^{-1}cm^{-1}$	$642.0 M^{-1}cm^{-1}$
ϵ_2	$498.8 M^{-1}cm^{-1}$	$514.9 M^{-1}cm^{-1}$
ϵ_3	$809.8 M^{-1}cm^{-1}$	$749.5 M^{-1}cm^{-1}$
ϵ_4	$120 M^{-1}cm^{-1}$	$120 M^{-1}cm^{-1}$
Sum of square	3.64×10^{-2}	5.84×10^{-3}
Correlation coefficient	0.967	0.998

Conclusion

It is known that thiol can reduce Mo(VI) to Mo(V)¹⁴ (Eq. (iv)). Furthermore, in Mo(VI) thiolate complexes, Mo-S bonds are weak and susceptible to hydrolysis.



Based on the above, it can reasonably be presumed that the native sulfite oxidase protein on purification and subjected to prolong standing in aqueous medium may respond to similar hydrolysis with the liberation of free sulfahydryl (SH) moiety. The reducing ability of the free cysteine thus liberated by hydrolysis may slowly interact with the left out intact Mo-cofactor of the protein. The chemistry involved there may be very similar to what we have shown in the present paper suggesting that there is a possibility of redox reaction where free thiol moiety can reduce Mo(VI) to Mo(IV). The reduced molybdenum is relatively stable and can withstand hydrolysis causing crystallisation of the system. Crystallisation procedure of the native protein under different buffering conditions can throw more light on the cause for its reduction during crystallization. Recently the influence of buffer composition has been shown to dictate the structural alteration of the native protein of DMSO class of reductase¹⁵. Thus, we suspect, based on the lability of

Mo(VI)-S bond, the related solution chemistry may be dictating the crystallisation process of the native protein.

Acknowledgement

We thank Department of Science and Technology, New Delhi, India for funding and IIT Kanpur for laboratory facilities.

References

- 1 McLeod R M, Farkas W, Fridovitch I & Handler P, *J Biol Chem*, 236 (1961) 1841; Cohen H L, Betcher-Lange S, Kessler D L & Rajagopalan K V, *J Biol Chem*, 247 (1972) 7759.
- 2 Johnson J L & Rajagopalan K V *J Biol Chem*, 252 (1977) 2017; Kipke C A, Cusanovitch M A, Tollin G, Sunde R A & Enemark J H *Biochemistry*, 27 (1988) 2918; Sullivan E P, Hazzard J T, Tollin G & Enemark, J H, *Biochemistry*, 32 (1993) 12465.
- 3 Kisker C, Shindelin H & Rees D C, *Annu Rev Biochem*, 66 (1997) 233; Hille R, *Chem Rev*, 96 (1996) 2757.
- 4 Rajagopalan K V, *Adv Enzymol Relat Areas Mol Biol*, 64 (1991) 215; Rajagopalan, K V & Johnson J L, *J Biol Chem*, 267 (1992) 10199.
- 5 Cramer S P, Gray H B & Rajagopalan K V, *J Am chem Soc*, 101 (1979) 2772; Cramer S P, Wahl R & Rajagopalan K V *J Am chem Soc*, 103 (1981) 7721.
- 6 George G N, Kipke C A, Prince R C, Sunde R A, Enemark J H & Cramer S P, *Biochemistry*, 28 (1989) 5075.
- 7 George G N, Garrett R M, Prince R C & Rajagopalan K V, *J Am chem Soc*, 118 (1996) 8588.
- 8 Garton S D, Garrett R M, Rajagopalan K V & Johnson M K, *J Am chem Soc*, 119 (1997) 2590.
- 9 Kisker C, Schindelin H, Pacheco A, Wehbi W A, Garrett R M, Rajagopalan K V, Enemark J E & Rees D C, *Cell*, 91(1997)1.
- 10 Das S K, Chaudhury P K, Biswas D & Sarkar S, *J Am chem Soc*, 116 (1994) 9061; Chaudhury P K, Das S K & Sarkar S, *Biochem J*, 319 (1996) 953.
- 11 Sarkar S, Sah R, Chaudhury P K, Maiti R & Das S K, *Proc Indian Acad Sci (Chem. Sci)* 107 (1995) 355.
- 12 Connors K A, *Chemical kinetics*, (VCH, New York) 1990.
- 13 Box G E P, Hunter W G & Hunter J S, *Statistics for experiments*, (John Wiley, New York) 1978.
- 14 Wedd A G, *Sulfur, its significance for chemistry, for the geo-, bio- and cosmosphere and technology. Studies in inorganic chemistry*, Vol. 5, edited by A Muller & B Krebs, (Elsevier, Amsterdam, Netherlands), 1984, pp. 181.
- 15 Schindelin H, Kisker C, Hilton J, Rajagopalan K V & Rees D C, *Science*, 272 (1996) 1615; Schneider F, Löwe J, Huber R, Schindelin H, Kisker C & Knäbelin J, *J mol Biol*, 263 (1996) 53; McAlpine A S, McEwan A G, Shaw A L & Bailey S, *J boil inorg Chem*, 2 (1997) 690.